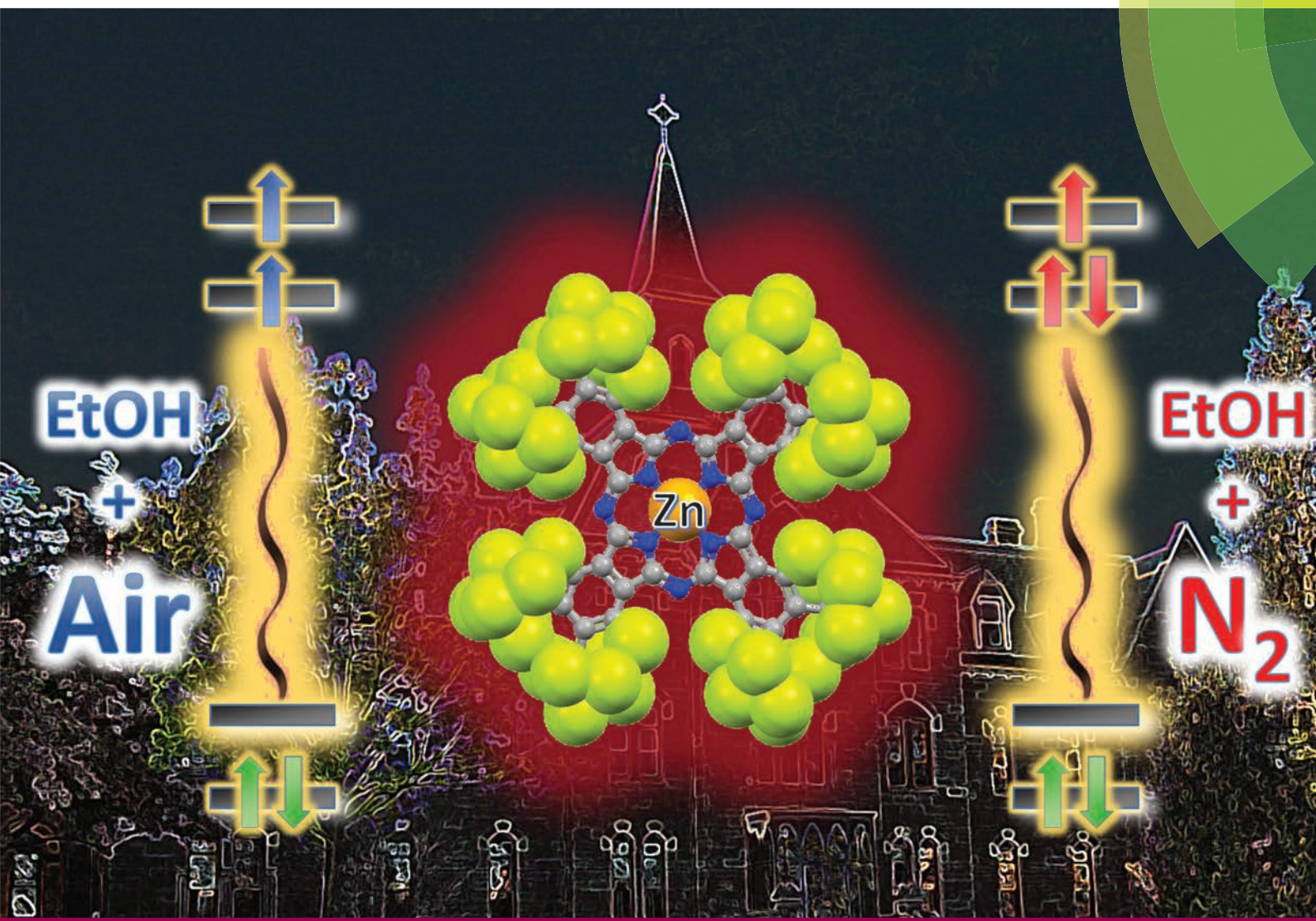
Volume 43 | Number 40 | 28 October 2014 | Pages 14911–15246

Dalton Transactions

An international journal of inorganic chemistry

www.rsc.org/dalton



Featuring the themed issue: Inorganic chemistry for renewable energy conversion and storage

ISSN 1477-9226

ROYAL SOCIETY OF CHEMISTRY

PAPER

Sergiu M. Gorun, Sabine Van Doorslaer *et al.*

Photoreduction and light-induced triplet-state formation in a single-site fluoroalkylated zinc phthalocyanine

Dalton Transactions

PAPER

View Article Online
View Journal | View Issue

Published on 22 April 2014. Downloaded by Library for Natural Sciences of the RAS on 9/3/2018 9:09:16 AM.

Cite this: *Dalton Trans.*, 2014, **43**, 14942

Photoreduction and light-induced triplet-state formation in a single-site fluoroalkylated zinc phthalocyanine†

Hans Moons,[a] Andrei Loas,[b,c] Sergiu M. Gorun*[b] and Sabine Van Doorslaer*[a]

Received 28th February 2014,
Accepted 22nd April 2014

DOI: 10.1039/c4dt00621f

www.rsc.org/dalton

Electron-withdrawing perfluoroalkyl peripheral substituents enhance the photosensitizing properties of metal phthalocyanines while increasing their solubility, thus providing opportunities for advanced characterization of their catalytically-relevant excited states. Optical absorption and electron paramagnetic resonance (EPR) spectroscopy experiments reveal that red light induces the reduction of perfluoroisopropyl-substituted zinc(II) phthalocyanine ($F_{64}PcZn$) dissolved in ethanol. A similar photoreduction does not occur in toluene. Furthermore, intense UV irradiation causes the photodegradation of $F_{64}PcZn$ in ethanol, but low power UV illumination favours the formation of the triplet excited state, a prerequisite for new photocatalytic applications. The UV-induced triplet state of $F_{64}PcZn$ is characterized using a combination of transient EPR experiments and DFT computations.

Introduction

Phthalocyanines (Pcs) are employed in a wide variety of applications.[1] Initially used as industrial dyes, they are currently investigated as state-of-the-art materials for implementation in molecular electronic devices, such as solar cells, or for use as photodynamic therapy agents. Moreover, the catalytic properties of these complexes are of interest.[2] The versatile phthalocyanine chemistry allows for fine tuning of their properties by variation of the Pc ring substituents and the central metal.[1] Previously, some of us have shown that by introducing perfluoroisopropyl (*i*-C_3F_7) peripheral substituents in the perfluorophthalocyanine ring to obtain 29*H*,31*H*,1,4,8,11,15,18,22,25-octafluoro-2,3,9,10,16,17,23,24-octakis-perfluoroisopropyl phthalocyanine ($F_{64}PcH_2$),[3,4] one can easily produce molecules containing (i) closed shell ions zinc[2a] and magnesium,[2b,c] (ii) open shell ions cobalt[5] and copper,[6] as well as (iii) double-decker, lanthanide complexes,[7] all of which yielded single crystals exhibiting long-range order. The enhanced solubility of these tridimensional perfluoroalkyl-perfluorophthalocyanines paved the way for many applications in catalysis[2,8–10] and photodynamic therapy.[4] Films and powders of different metal $F_{64}Pcs$ exhibit only a small extent of intermolecular electronic coupling.[6,11] This single-site isolation favors catalytic applications: $F_{64}PcZn$ (Fig. 1), for instance, is able to oxygenate external substrates,[9] or, intercalated in bentonite as a hybrid photosensitizer, oxidatively degrade Acid Orange 7 in aqueous solutions under visible light.[8]

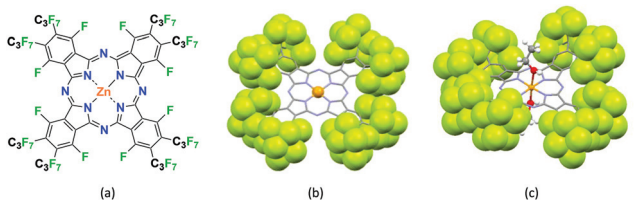


Fig. 1 (a) Structural formula of $F_{64}PcZn$; C_3F_7 = perfluoroisopropyl. (b) X-ray structure of $F_{64}PcZn(acetone)_2$.[5] The axially coordinated acetone molecules have been omitted for the sake of clarity. (c) DFT-generated $F_{64}PcZn(ethanol)_2$. Color code: F, green, N, blue, C, gray, O, red, H, white. The F atoms are shown as van der Waals, spheres, and the rest of the macrocycle atoms, with the exception of the Zn atom, are depicted as capped sticks. The Zn atom and the axial ligands are shown in ball-and-stick representation.

The triplet spin state of photoexcited $F_{64}PcZn$ was shown to be sufficiently long living to render the complex a potential photosensitizer.[5] In the absence of dioxygen, the lifetime of this state was found to be ~50 times longer than that of the perfluorinated analogue containing only F atoms, $F_{16}PcZn$, the key reason being most likely the lack of aggregation of the former complex, in contrast to the latter.

[a]*University of Antwerp, Department of Physics, Universiteitsplein 1, 2610 Antwerp, Belgium. E-mail: sabine.vandoorslaer@ua.ac.be*
[b]*Center for Functional Materials and Department of Chemistry and Biochemistry, Seton Hall University, South Orange, NJ 07079, USA. E-mail: sergiu.gorun@shu.edu*
[c]*Department of Chemistry, Massachusetts Institute of Technology, Cambridge, MA 02139, USA*

†Electronic supplementary information (ESI) available: Electronic spectra of $F_{64}PcZn$, UV degradation experiments, kinetic and structural modeling data, structural parameters of ZnN_2O_2 and ZnN_4 chromophores, and DFT results. See DOI: 10.1039/c4dt00621f

This journal is © The Royal Society of Chemistry 2014

Published on 22 April 2014. Downloaded by Library for Natural Sciences of the RAS on 9/3/2018 9:09:16 AM.

The formation of excited states is a key step toward reactivity and, therefore, their physical parameters are worth investigating. Amongst useful techniques, transient electron paramagnetic resonance (TREPR) is known to be a versatile tool to monitor the formation of photo-induced triplet states and radical pairs,[12,13] and was used to identify and characterize the triplet state of photoexcited H_{16}PcZn, the parent, H-containing phthalocyanine, both in a frozen solution in 2-methyltetrahydrofuran and in powder form at low temperatures.[14]

We report the use of W-band TREPR in combination with density functional theory (DFT) computations to characterize paramagnetic species obtained from F_{64}PcZn following irradiation, *viz.* its triplet state generated *via* photoexcitation in frozen solutions and the $[F_{64}PcZn]^{\bullet-}$ radical anion generated *via* photoreduction.

The anion radical was reported to have been obtained *via* the electrochemical reduction of F_{64}PcZn or *via* its photochemical reduction using sacrificial hydrazine hydrate.[15,16] In the current work, we show that the photochemical production of reactive radical species can be achieved in ethanol without the need for an external electron donor, an observation relevant to the previously reported photocatalytic properties of F_{64}PcZn in ethanol.[9]

Experimental

Materials

Zinc(II) 1,4,8,11,15,18,22,25-octafluoro-2,3,9,10,16,17,23,24-octakisperfluoroisopropyl-perfluorophthalocyanine (F_{64}PcZn) was obtained and purified as described previously.[5] For EPR measurements, absolute ethanol (Sigma-Aldrich) solutions of 1 mM F_{64}PcZn were prepared. For optical absorption measurements, the solution were diluted sufficiently to exhibit optical absorbance values below 2.

Optical absorption spectroscopy

UV-visible electronic absorption measurements were carried out on a Varian Cary 500 UV-Vis-NIR spectrophotometer using 1 cm quartz cells. If anaerobic conditions were required, the samples were prepared, transferred into the quartz cell and sealed in a glove box under a purified N_2 atmosphere. For the photoreduction experiments, the samples were irradiated with a 450 W Xe lamp (Edinburgh Instruments Xe900) prior to UV-visible absorption measurements. For the red light illumination, the Xe900 lamp was used with a 570 nm cut-off filter.

X-band continuous-wave EPR experiments

For the X-band CW EPR measurements, a Bruker ESP300E spectrometer (microwave frequency ~9.4 GHz) was used. The static magnetic field (0–1.5 T) was provided by a Varian V-7300 electromagnet. The field value was measured using a Bruker ER035M NMR gauss meter. The resonator was a Bruker ER 4102ST rectangular cavity operating in the TE_{102} mode. A modulation amplitude of 0.1 mT and a microwave power of 2 mW were used for the room-temperature experiments.

W-band transient EPR experiments

The W-band transient EPR experiments were performed at 50 K using a Bruker ELEXSYS E680 spectrometer equipped with a continuous helium flow cryostat and a superconductive split-coil magnet (0–6 T, Oxford Instruments). The light source was a Nd:YAG laser (QuantaRay INDI, Spectra Physics, pulse width ~5 ns) operated in Q-switched mode at a 20 Hz repetition rate at 355 nm. The light was transported through a high-power silica fiber resulting in a power of approximately 0.25 mJ per pulse on the sample location. The EPR spectra were simulated using EasySpin, a Matlab toolbox.[17]

DFT computations

Spin-unrestricted DFT computations were performed using the ORCA package.[18–21] Two F_{64}PcZn species were modeled. Model A is the triplet state of F_{64}PcZn in ethanol (no solvation) while Model B is the triplet state of the bis solvated species, F_{64}PcZn-(ethanol)$_2$. Fig. 1b represents graphically Model A based on the F_{64}PcZn(acetone)$_2$ structure with the axial ligands omitted. Fig. 1c represents Model B based on the DFT coordinates. In order to simulate the solvent environment, a dielectric medium with the dielectric constant of ethanol according to the COSMO model was used.[22] For the geometry optimizations, the Becke–Perdew density functional (BP86)[23–25] was used together with the resolution of the identity method.[26–28] The split-valence plus polarization (SVP) basis set[29] was used for all atoms except for the zinc atom, in which case a more polarized triple zeta valence (TZVPP) basis was employed. The energy converged to 10^{-8} Hartree (Eh), with the convergence tolerances in the geometry optimization of 3×10^{-4} Eh Bohr^{-1} for the gradient and 5×10^{-6} Eh for the total energy. No symmetry constraints were used for the structure optimization. Single point calculations with the B3LYP functional[30] were carried out at the optimized geometries to predict the EPR spectral parameters. In these calculations, the "EPR-II" basis set[31] was used for all atoms, except for the zinc ion, for which the (TZVPP) basis set was used. The zero-field splitting tensor was calculated taking the spin–spin interaction and the spin–orbit coupling into account.

Results and discussion

Photo-stability and photo-reduction of F_{64}PcZn

The steady-state optical absorption spectra of F_{64}PcZn in ethanol recorded in air (Fig. S1†) and under a N_2 atmosphere (Fig. 2) are similar to those previously reported for F_{64}PcZn in DMF.[15,16] When ethanolic solutions of F_{64}PcZn were irradiated with UV light generated by a Xe lamp (450 W), a clear decrease in absorbance was observed under aerobic conditions, Fig. S2;† after 60 min of irradiation, the absorbance was reduced to about 80% of the original signal intensity. The limited stability of metal phthalocyanines under UV light has

Published on 22 April 2014. Downloaded by Library for Natural Sciences of the RAS on 9/3/2018 9:09:16 AM.

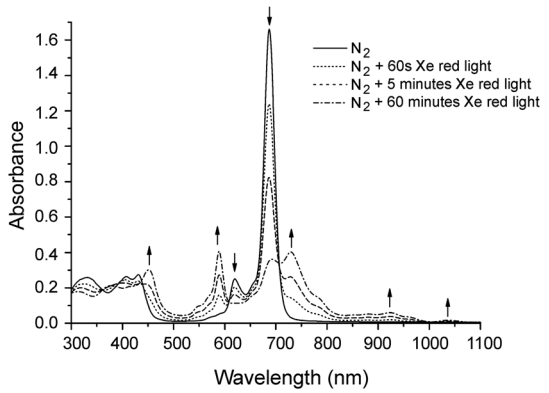


Fig. 2 Steady-state UV-visible spectra of $F_{64}PcZn$ in ethanol under a N_2 atmosphere (solid line) and after successive irradiation with a 450 W Xe lamp equipped with a cut-off filter at 570 nm.

Table 1 Comparison of the absorption maxima of $[F_{64}PcZn]^{\bullet-}$ obtained *via* different reduction methods in ethanol and DMF

λ_{max} (nm)	
Photoreduced $F_{64}PcZn$ in ethanol (this work)	Photo-/electrochemically reduced $F_{64}PcZn$ in DMF[16]
452	468
589	594
729	743
924	Not reported
1038	Not reported

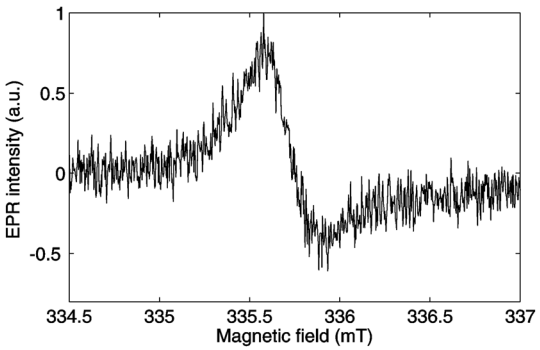


Fig. 3 Room temperature X-band CW EPR spectrum of the radical signal obtained under a N_2 atmosphere immediately after illumination with red light of $F_{64}PcZn$ in ethanol.

been reported earlier.[32,33] Under these conditions, the stability of $F_{64}PcZn$ in ethanol can be considered good, given that some phthalocyanines are reported to almost fully degrade within an hour as a result of scattered daylight.[32] For instance, 30 minutes of illumination of a $F_{16}PcZn$ solution in toluene in air resulted in only ~30% retention of the original signal intensity (not shown).

When the UV component of the Xe lamp radiation was filtered out with the aid of a 570 nm cut-off filter, illumination of an oxygen-free solution of $F_{64}PcZn$ in ethanol produced a surprising change in the absorption spectrum, identified as a photo-reduction to the ring-reduced radical anion species $[F_{64}PcZn]^{\bullet-}$ (Fig. 2). The latter was assigned based on previously reported absorption bands characteristic of this species (upward arrows, Fig. 2), which were also observed for the electrochemically reduced complex and the photo-reduced complex in the presence of sacrificial hydrazine hydrate[15,16] (Table 1). The small hypsochromic shifts of the absorption maxima are due to the change of solvent. The photoreduction was found to be reversible: after oxygenation of the sample the initial optical spectrum of $F_{64}PcZn$ in ethanol is regenerated (Fig. S3†). The experiment was repeated with full spectrum UV-visible light (450 W Xe lamp, Fig. S5a†). In contrast to the relatively slow build-up of $[F_{64}PcZn]^{\bullet-}$ observed under red-filtered light (Fig. 2 and S4†), complete photoreduction occurs within the first 3 minutes under UV illumination (Fig. S5†). However, in this case, a slow $F_{64}PcZn$ degradation also takes place. When $F_{64}PcZn$ is dissolved in toluene, no reduction upon red light activation is observed (Fig. S6†).

The formation of the radical anion $[F_{64}PcZn]^{\bullet-}$ was further probed *via* EPR. Fig. 3 shows the X-band CW-EPR spectrum of an anaerobic ethanol solution of red light-photoreduced $F_{64}PcZn$. A featureless signal around $g = 2.003$ is noted, typical of a radical and similar to the signal observed for $[F_{64}PcZn]^{\bullet-}$ generated photochemically in DMF in the presence of hydrazine hydrate.[16] This result confirms that phthalocyanine ring reduction has occurred.

Electrochemical studies on metallophthalocyanines have shown that up to four electrons can be reversibly added to, or up to two electrons can be reversibly removed from the Pc macrocycle.[34] To the best of our knowledge, photoreduction of a zinc phthalocyanine using the solvent (ethanol) as the electron donor has never been reported before.

Earlier cyclic voltammetry studies have shown that $F_{64}PcZn$ can be reduced electrochemically much easier than PcZn.[16] The facile photoreduction of $F_{64}PcZn$ in the presence of ethanol may be explained by an exacerbated Lewis acidity of the Zn ion induced by the electron-withdrawing perfluoroalkyl peripheral substituents, thus rendering the metal centre prone to axial coordination of ethanol ligands. This is in line with our earlier pulsed EPR studies on $F_{64}PcCu$ that unambiguously proved binding of ethanol to this Cu(II) complex in solution.[6] The coordination of ethanol may make an efficient inner-sphere electron transfer process possible, thus favouring the reduction of the complex.

The observation that a reduction does not take place for the complex in a non-coordinating solvent, like toluene (Fig. S6†), suggests that axial ligation indeed plays a crucial role in this process. The need for coordination of ethanol to the zinc phthalocyanine may also explain why the formation of $[F_{64}PcZn]^{\bullet-}$ under red light illumination cannot be modeled by a mono-exponential fit (Fig. S4†). No reduction of the complex is observed in any solvent when oxygen is present. When air is contacted with either the red light- or UV-reduced samples, the restoration of the original optical spectrum takes place, but several hours are needed to reach completion (Fig. S7†). This

 This journal is © The Royal Society of Chemistry 2014

Published on 22 April 2014. Downloaded by Library for Natural Sciences of the RAS on 9/3/2018 9:09:16 AM.

observation suggests that the lack of detectable reduction under aerobic illumination is not due to the fast re-oxidation of $[F_{64}PcZn]^{\bullet-}$ to $F_{64}PcZn$ (with the corresponding formation of O_2^{-}). Competitive reactions involving dioxygen seem to hamper $[F_{64}PcZn]^{\bullet-}$ formation, rather than quenching of the radical state. Most likely, the competing reaction is the efficient production of singlet oxygen, $^1O_2$, *vide infra*.

Triplet excited state formation

As mentioned above, $F_{64}PcZn$ degrades in air under UV illumination, although its UV-stability is remarkably better than that reported for other zinc phthalocyanines. Earlier studies on PcZn and other metallophthalocyanines suggested that the following photochemical processes may be responsible for the photodegradation in air:[32] (i) the phthalocyanine complex is excited from the S_0 to the S_1 state, which can be converted *via* inter-system crossing (ISC) to a triplet state (T_1), and (ii) the T_1 state reacts with ground-state oxygen, $^3O_2$, to produce $^1O_2$ that may subsequently oxidize the macrocycle. A triplet excited state with a lifetime of 52 μs was determined following anaerobic red light illumination of 10 μM $F_{64}PcZn$ in acetone.[5] In the presence of oxygen, $^1O_2$ is formed and higher tumor regression was observed during photodynamic therapy upon application of lower doses of a photosensitizer when comparing $F_{64}PcZn$ and PcZn *in vivo*.[5] Furthermore, $F_{64}PcZn$ is a much more efficient catalyst in the photooxidation of citronellol compared with other zinc phthalocyanines studied, owing to both its high quantum yield of $^1O_2$ production and high photostability.[9]

In order to investigate whether the T_1 state is also induced in $F_{64}PcZn$ under UV illumination, we performed transient EPR experiments. These measurements also allow for a determination of the spin Hamiltonian parameters of the T_1 state of $F_{64}PcZn$.

Although photodecomposition was observed under strong UV irradiation, low-temperature TREPR experiments could be performed with negligible degradation when exciting the molecule at 355 nm with a relatively low power laser light. Indeed, at low temperature, the diffusion rate of oxygen into the solution, which could be responsible for the quenching of the radical, is reduced and the magnetization dephasing occurs on a much faster time scale than oxygen diffusion.[14]

Fig. 4 shows the photo-excited triplet state of $F_{64}PcZn$ in ethanol detected at 50 K with W-band TREPR. The spectrum may also be simulated, including the electron Zeeman term and the zero-field splitting assuming the spin Hamiltonian:

$$\hat{H} = \beta_e B_0 g \hat{S} + D\left(\hat{S}_z{}^2 - \frac{1}{3}\hat{S}^2\right) + E(\hat{S}_x{}^2 - \hat{S}_y{}^2) \qquad (1)$$

The g-tensor has principal values g_x, g_y and g_z, B_0 is the external magnetic field, β_e is the Bohr magneton and D and E are the zero-field parameters. The best fit parameters are reported in Table 2, while the simulation is shown in Fig. 4. The population distribution of the levels is set to 0 : 0 : 1 for $p_x : p_y : p_z$ in the simulation. D is assumed to be positive in accordance with the parent PcZn[14] and E is also taken positive

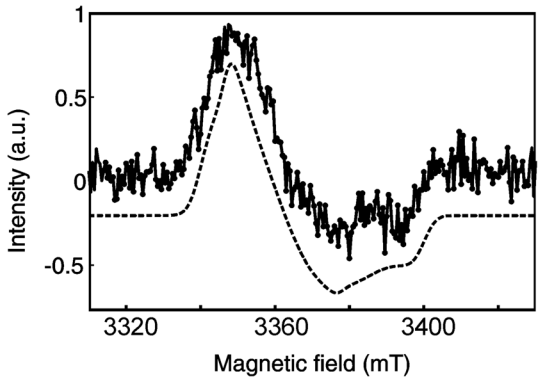


Fig. 4 W-band transient EPR spectrum of $F_{64}PcZn$ in ethanol at 50 K (solid line) and its simulation (dashed line), taken ~1.5 μs after photo-excitation with a laser flash at 355 nm.

in the simulation. The values are of the same order of magnitude as those earlier observed for solutions of the parent PcZn and other zinc phthalocyanines and porphyrins[14,35,36] (Table 2). In the frozen solution, the T_1 state of $F_{64}PcZn$ is formed *via* the conventional ISC process from the S_1 state. The population distribution indicates a preferential occupation of the lowest out-of-plane sublevel, provided that the zero-field splitting axes and the g tensor axes coincide. A dominant ISC to the out-of-plane sublevels was also reported.[35]

The D values of metal Pcs are generally lower than those of the corresponding porphyrin complexes due to an extended delocalization of the unpaired π electrons in the T_1 state.[35] The D value of the triplet state of $F_{64}PcZn$ is, however, higher than those found for other metal Pcs (Table 2). It has been shown earlier that axial ligation may influence the zero-field splitting parameters of metal porphyrins.[35] Ethanol ligation may thus be responsible for the increased D value observed for the T_1 state of $F_{64}PcZn$, although the effect of the electron-withdrawing perfluoroalkyl substituents could also play a role.

In order to elucidate this further, DFT computations of the spin Hamiltonian parameters of the triplet state of $F_{64}PcZn$ in ethanol (Model A) and of $F_{64}PcZn(ethanol)_2$ in ethanol (Model B) were performed. The computed g values and zero-field splitting parameters are shown in Table 2, along with the experimental ones.

The spin density distribution (Fig. 5) of the triplet state of Model B explains the small, but non-negligible E value. The 4-fold axis is lost but two orthogonal mirror planes containing the O(ethanol)–Zn–O(ethanol) axis are noted.

Surprisingly, although smaller than the equivalent value for Model B, the computed E value of Model A was also not zero. Since no symmetry constraints were imposed during the geometry optimization, small differences in the *i*-C_3F_7 substituents rotational positions, which break the symmetry, may contribute to the non-zero E value. It should be noted that DFT computations on the singlet and triplet states of PcZn also showed a decrease in symmetry from D_{4h} (ground state S_0) to D_{2h} in the triplet state.[37] In fact, all reported experimental E values for zinc phthalocyanines (Table 2) are non-zero.

Published on 22 April 2014. Downloaded by Library for Natural Sciences of the RAS on 9/3/2018 9:09:16 AM.

Table 2 Experimental and DFT-computed *g*-values, zero-field splitting parameters for the T_1 state of $F_{64}PcZn$ in ethanol compared with other complexes, and structural comparison of experimental and modelled $F_{64}PcZn$ parameters

Complex	g_x	g_y	g_z	$\|D\|$ (cm^{-1})	$\|E\|$ (cm^{-1})	Reference/ method	Macrocycle angles (°)	Zn–N bond lengths (Å)	Zn–O (axial) bond length (Å)
$F_{64}PcZn$ in ethanol	2.002[a]	2.000[a]	1.997[a]	0.028[b]	0.003[b]	This work/TREPR	179.9[c,e] 0.0[d,e]	2.007 ± 0.003[e]	2.422 ± 0.003[e]
$F_{64}PcZn$ (Model A)	2.0032	2.0028	1.9978	0.0229	0.0011	This work/DFT	177.8 ± 0.2[c,e] 4.7 ± 0.6[d,e]	2.012 ± 0.008	—
$F_{64}PcZn(EtOH)_2$ (Model B)	2.0032	2.0028	2.0004	0.0242	0.0037	This work/DFT	176 ± 1[c,e] 21 ± 1[d,e]	2.04 ± 0.01	2.310
PcZn in 2-methyl-THF	2.008	2.004	2.002	0.025	0.004	14/TREPR	—	—	—
tbPcZn[f] in Tol : $CHCl_3$	n.r.	n.r.	n.r.	0.024	0.005	35/TREPR	—	—	—
$tbPcH_2$[f] in Tol : $CHCl_3$	n.r.	n.r.	n.r.	0.025	0.002	35/TREPR	—	—	—
ZnTPP[g] in Tol : $CHCl_3$	n.r.	n.r.	n.r.	0.031	0.009	36/TREPR	—	—	—

[a] Experimental error = 0.001. [b] Experimental error = 0.002 cm^{-1}. [c] The average of the 2 Ct–Zn–Ct angles, where Ct are the geometric centers of the *trans* benzene rings. [d] The average of the dihedral angles made by *trans* benzene rings. [e] These experimental values refer to the isoelectronic $F_{64}PcZn(acetone)_2$.[5] [f] tbPc = tetra-tertbutyl phthalocyanine. [g] TPP = tetraphenylporphyrin; Tol = toluene; n.r. = not reported.

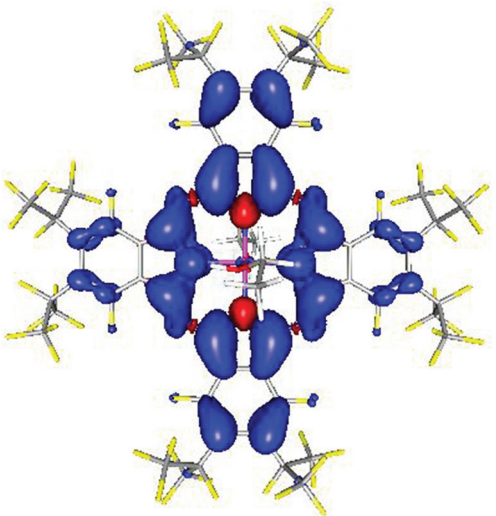


Fig. 5 Spin density distribution of the triplet state of $F_{64}PcZn(ethanol)_2$ in ethanol, Model B, viewed along the O(ethanol)–Zn–O(ethanol) axis. Blue: positive spin density; red: negative spin density.

Perhaps more importantly than the break of the D_{4h} symmetry due to the restricted rotations of the *i*-C_3F_7 groups, Pc ring distortions may be anticipated due to axial coordination. The geometrical features of Models A and B reveal the anticipated distortions. Thus, a comparison of the calculated geometries, based on the coordinates of the optimized geometries (see the ESI†) and the experimental observations for $F_{64}PcZn(acetone)_2$, Fig. S9 and Table S1,† reveals that the DFT-generated geometry of the $F_{64}PcZn(ethanol)_2$ complex exhibits a saddle distortion (Fig. 1c). One can estimate the macrocycle distortions by computing their Ct–Zn–Ct angles, where Cts are the geometric centers of *trans* benzene rings. For lack of distortions, the angle should be 180°, as is indeed observed for $F_{64}PcZn(acetone)_2$, Table 2. In contrast, this angle is 177.8 ± 0.2 and 176 ± 1° for Models A and B, respectively, proving the existence of saddle distortions. A second type of distortion, which also affects the degree of π conjugation, is represented by the dihedral angles made by the *trans* benzene rings. While this distortion is absent in $F_{64}PcZn(acetone)_2$, it is about 5° in Model A, which lacks axial ligands. In contrast, Model B, which displays bis axial ethanol coordination, Fig. 1c, exhibits a severe distortion, 21°, thus breaking the 4-fold axial symmetry. Notably, ethanol coordination also distorts the ZnN_4 chromophore of Model B relative to that of both Model A and the similarly coordinated $F_{64}PcZn(acetone)_2$ as illustrated by the goodness-of-fit of the overlaid structures, Fig. S9 and Table S1.† The effects of bis axial coordination are difficult to assess accurately, since there are no *trans* bis acetone or ethanol complexes reported in the Cambridge Crystallographic Database (2014), with the exception of $F_{64}PcZn(acetone)_2$.[5] A review of axially ligated acetone and ethanol complexes exhibiting either equatorial N_4 or N_2O_2 coordination, Tables S2 and S3,† reveals in both cases a lengthening of the Zn–O bond by ~0.06 Å on going from acetone to ethanol, reaching an average of 2.20 Å. The corresponding, larger value of 2.445 Å encountered in $F_{64}PcZn(acetone)_2$ is likely due to the addition of the sixth, *trans* ligand. This addition and the resulting *trans* effect suggest that the ethanol ligand is labile. The symmetry features, taken together, establish the origin of the spin density distribution mostly in the Pc ring distortions, given that the tertiary F groups are out of the Pc plane in Models A and B removing the mirror symmetry elements.

The computed zero-field splitting parameters in Table 2 agree well with the observed experimental values, and the DFT computations suggest that axial ligation indeed leads to a larger *D* value. However, one has to be careful when relying too strongly on a quantitative comparison between DFT and experimental results, since the agreement may be coincidental; DFT computation of zero-field splitting parameters for transition metals remains problematic.[38–40] Present-day DFT methods rely on spin-unrestricted single-determinant methods, which are reasonably accurate for one-electron spin-dependent properties. However, they do not accurately reproduce the two-electron spin-dependent properties like the zero-field splitting.[41] Yet, the geometrical predictions of the DFT calculations are consistent with the experimental observations.

 This journal is © The Royal Society of Chemistry 2014

Published on 22 April 2014. Downloaded by Library for Natural Sciences of the RAS on 9/3/2018 9:09:16 AM.

For an accurate calculation of zero-field splitting parameters, it is necessary to use correlated *ab initio* methods, which is beyond the scope of this contribution. Note that, even though the symmetry of the *g* tensor was correctly predicted, its principal values deviate significantly from the experimental ones, illustrating further the inherent difficulties in performing reliable DFT computations.

In this respect, it is interesting to note that the experimental g_z value of the T_1 state of F_{64}PcZn in ethanol is considerably lower than the free-electron *g* value (2.0023). This was not observed for PcZn in 2-methyl-THF.[14] In fact, also the average isotropic *g* value is larger in the latter case. Although it is unclear at present what causes this difference, we should remark that the measurements in ref. 14 were performed at X-band, resulting in a reduced *g* resolution and a larger experimental error on the principal *g* values than when W-band microwave frequencies are used. Furthermore, although one should be careful when performing quantitative comparisons between experiment and DFT (*vide supra*), a g_z value below 2.0023 was predicted for both Models A and B (Table 2), suggesting that this is an intrinsic property of the system under study.

Consequences for applications

Our observation that F_{64}PcZn can be anaerobically reduced by red light in the presence of only ethanol is unprecedented for phthalocyanines. Photoreduction has been observed for other phthalocyanines, but always in the presence of strong electron donors, such as azaferrocene, hydrazine and different amines.[16,42–44] The possibility of anaerobically reducing a Pc ring in the presence of an alcohol (in other words, oxidizing the solvent) opens new reactivity pathways. Simple oxygenation restores the neutral F_{64}PcZn molecule.

The related F_{64}PcCo complex has already been shown to exhibit unusual chemistry, being able to catalytically reduce oxygen[10] and couple phosphanes with acetone to form ylides.[2a] Key to this unusual behavior seems to be the electron-withdrawing effect of the *i*-C_3F_7 peripheral substituents. These substituents not only render the complexes readily soluble in organic solvents, but also favor axial binding to the central metal of ligands with lower coordinating power, such as alcohols.

Although F_{64}PcZn dissolved in ethanol was found to degrade in air under strong UV irradiation, its stability is much improved with respect to other phthalocyanines and does not affect its favorable catalytic properties.[9] Earlier studies indicated that both the molecular structure and the solvent play a crucial role in UV stability.[32] The bridging aza nitrogen atoms form the weakest point in the Pc ring. Effective σ-donors were found to raise the electron density of the conjugated C–N bonding system and enhance the chemical stability.[32] Ethanol ligation may thus actively promote the UV stability of the F_{64}PcZn complex.

Finally, zinc phthalocyanines and porphyrins have been long contemplated as photosensitizers for medical applications.[45] A good candidate in this field has to fulfill several key requirements, including high stability, high solubility, low photodegradation, low toxicity and an efficient formation of the T_1 state leading to evolution of $^1O_2$. The excited triplet state of F_{64}PcZn forms readily and bears similar zero-field splitting parameters to other Pc and porphyrin derivatives, but has the added advantage of improved solubility in polar solvents.

Conclusions

In an oxygen-free environment, F_{64}PcZn is readily reduced in ethanol under red light illumination, a rare phenomenon not encountered for other metallophthalocyanine analogues or in non-coordinating solvents, such as toluene. The photoreduction of the phthalocyanine ring is facilitated by axial ligation of ethanol, a process mediated by the strong electron-withdrawing effects of the perfluoroalkyl peripheral substituents, which enhance the Lewis acidity of the central metal.

Although intense UV illumination leads to the photodegradation of the complex in ethanol, photostability is greatly enhanced compared with related PcZn derivatives. The photoexcited T1 state of F_{64}PcZn in ethanol has zero-field parameters that are indicative of axial ethanol ligation, consistent with DFT calculations of spin density distributions on solvated and unsolvated model complexes, as well as with a bis-ligated solid-state X-ray structure. The possibility of anaerobically and reversibly reducing the Pc ring while subsequently oxidizing substrates may open new avenues in catalytic chemistry.

Acknowledgements

Partial support from the National Science Foundation (SMG) is gratefully acknowledged.

Notes and references

1 N. B. McKeown, *Phthalocyanine Materials*: Synthesis, Structure and Function, Cambridge University Press, Cambridge, 1998.
2 (*a*) B. A. Bench, W. W. Brennessel, H.-J. Lee and S. M. Gorun, *Angew. Chem., Int. Ed.*, 2002, **41**, 750; (*b*) S. V. Dugan, Ł. Łapok, P. Zimcik, V. Novakova, A. Tochtenhagen, M. Hintsche, C. Litwinski, B. Roder, H. Patel and S. M. Gorun, Pub. #228, 245th ACS National Meeting, New Orleans, April 7–11, 2013; (*c*) S. V. Dugan, Ł. Łapok, A. Tochtenhagen, M. Hintsche, C. Litwinski, B. Roder, H. Patel, K. A. Griswold, J. Zunino and S. M. Gorun, to be submitted.
3 H.-J. Lee, W. W. Brennessel, J. A. Lessing, W. W. Brucker, V. G. Young and S. M. Gorun, *Chem. Commun.*, 2003, 1576.
4 R. Minnes, H. Weitman, H.-J. Lee and S. M. Gorun, *Photochem. Photobiol.*, 2006, **82**, 593.

Published on 22 April 2014. Downloaded by Library for Natural Sciences of the RAS on 9/3/2018 9:09:16 AM.

5 B. A. Bench, A. Beveridge, W. M. Sharman, G. J. Diebold, J. E. Van Lier and S. M. Gorun, *Angew. Chem., Int. Ed.*, 2002, **41**, 748.
6 H. Moons, Ł. Łapok, A. Loas, S. Van Doorslaer and S. M. Gorun, *Inorg. Chem.*, 2010, **49**, 8779.
7 M. Gonidec, I. Krivokapic, J. Vidal-Gancedo, E. S. Davies, J. McMaster, S. M. Gorun and J. Veciana, *Inorg. Chem.*, 2013, **52**, 4464.
8 D. Drozd, K. Szczubiałka, Ł. Łapok, M. Skiba, H. Patel, S. M. Gorun and M. Nowakowska, *Appl. Catal., B*, 2012, **125**, 35.
9 R. Gerdes, Ł. Łapok, O. Tsaryova, D. Wöhrle and S. M. Gorun, *Dalton Trans.*, 2009, 1098.
10 A. Loas, R. Gerdes, Y. Zhang and S. M. Gorun, *Dalton Trans.*, 2011, **40**, 5162.
11 C. Keil, O. Tsaryova, C. Himcinshi, D. Wöhrle, O. R. Hild, D. R. T. Zahn, S. M. Gorun and D. Schlettwein, *Thin Solid Films*, 2009, **517**, 4379.
12 P. Atkins, K. McLauglan and P. Percival, *Mol. Phys.*, 1973, **25**, 281.
13 A. van der Est, *Photosynth. Res.*, 2009, **102**, 335.
14 A. Barbon, M. Brustolon and E. E. van Faassen, *Phys. Chem. Chem. Phys.*, 2001, **3**, 5342.
15 S. P. Keizer, W. Han and M. J. Stillman, *Inorg. Chem.*, 2002, **41**, 353.
16 S. P. Keizer, J. Mack, B. A. Bench, S. M. Gorun and M. J. Stillman, *J. Am. Chem. Soc.*, 2003, **125**, 7067.
17 S. Stoll and A. Schweiger, *J. Magn. Reson.*, 2006, **178**, 42.
18 F. Neese, *J. Chem. Phys.*, 2001, **115**, 11080.
19 F. Neese, *J. Phys. Chem. A*, 2001, **105**, 4290.
20 F. Neese, *J. Chem. Phys.*, 2003, **118**, 3939.
21 F. Neese, *J. Chem. Phys.*, 2005, **122**, 034107.
22 S. Sinnecker, A. Rajendran, A. Klamt, M. Diedenhofen and F. Neese, *J. Phys. Chem. A*, 2006, **110**, 2235.
23 A. D. Becke, *Phys. Rev. A*, 1988, **38**, 3098.
24 J. P. Perdew, *Phys. Rev. B: Condens. Matter*, 1986, **33**, 8822.
25 J. P. Perdew, *Phys. Rev. B: Condens. Matter*, 1986, **34**, 7406.
26 B. I. Dunlap, J. W. D. Connolly and J. R. Sabin, *J. Chem. Phys.*, 1979, **71**, 3396.
27 K. Eichkorn, O. Treutler, H. Ohm, M. Haser and R. Ahlrichs, *Chem. Phys. Lett.*, 1995, **240**, 283.
28 O. Vahtras, J. Almlof and M. W. Feyereisen, *Chem. Phys. Lett.*, 1993, **213**, 514.
29 A. Schäfer, H. Horn and R. Ahlrichs, *J. Chem. Phys.*, 1992, **97**, 2571.
30 P. J. Stephens, F. J. Devlin, C. F. Chabalowski and M. J. Frisch, *J. Phys. Chem.*, 1994, **98**, 11623.
31 V. Barone, *Recent Advances in Density Functional Methods*, World Scientific Publ. Co., Singapore, 1996.
32 R. Słota and G. Dyrda, *Inorg. Chem.*, 2003, **42**, 5743.
33 T. Caronna, C. Colleoni, S. Dotti, F. Fontana and G. Rosace, *J. Photochem. Photobiol., A*, 2006, **184**, 135.
34 J. Mack and M. J. Stillman, *Inorg. Chem.*, 1997, **36**, 413.
35 K. Ishii, S. Abiko and N. Kobayashi, *Inorg. Chem.*, 2000, **39**, 468.
36 K. Akiyama, S. Terokubota and Y. Ikegami, *Chem. Phys. Lett.*, 1991, **185**, 65.
37 L. T. Ueno, C. C. Jayme, L. R. Silva, E. B. Pereira, S. M. de Oliveira and A. E. H. Machado, *J. Braz. Chem. Soc.*, 2012, **23**, 2237.
38 F. Neese, *Coord. Chem. Rev.*, 2009, **253**, 526.
39 *Calculation of NMR and EPR Parameters. Theory and Applications*, ed. M. Kaupp, M. Bühl and V. G. Malkin, Wiley-VCH Verlag, Weinheim, 2004.
40 F. Neese, *J. Biol. Inorg. Chem.*, 2006, **11**, 702.
41 M. van Gastel, *J. Chem. Phys.*, 2009, **131**, 7.
42 Y. Kaneko, T. Arai, H. Sakuragi, K. Tokumaru and C. Pac, *J. Photochem. Photobiol., A*, 1996, **97**, 155.
43 Y. Kaneko, Y. Nishimura, T. Arai, H. Sakuragi, K. Tokumaru and D. Matsunaga, *Photochem. Photobiol., A*, 1995, **89**, 37.
44 J. Zakrzewski and C. Giannotti, *Inorg. Chim. Acta*, 1995, **232**, 63.
45 *Photosensitizers in Medicine, Environment and Security*, ed. T. Nyokong and V. Ahsen, Springer Science, London, 2012.

 This journal is © The Royal Society of Chemistry 2014